Calculation of Phonon Frequencies and Thermodynamic Properties of Crystalline bcc Helium*

F. W. DE WETTE
Physics Department, University of Texas, Austin, Texas
and
Solid State Science Division, Argonne National Laboratory, Argonne, Illinois
AND
L. H. NOSANOW,
School of Physics and Astronomy, University of Minnesota, Minneapolis, Minnesota
AND
N. R. WERTHAMER
Bell Telephone Laboratories, Murray Hill, New Jersey
(Received 18 May 1967)

The lattice dynamics of crystalline bcc helium is treated by using the time-dependent Hartree approximation together with the results of variational calculations of the ground-state energy using correlated trial wave functions. The phonon spectrum has been calculated for various densities of bcc He^3 and He^4. We present dispersion curves, density-of-states histograms, and sound velocities for selected densities. In addition we have calculated (for these densities) the mean-square displacement and the specific heat C_V which is expressed as a temperature-dependent Debye temperature $\Theta(T)$. It is found that the reduced Θ-T relationships follow a universal curve for all densities considered. This is a theoretical confirmation of the experimental fact that the bcc phase of crystalline helium (like the other crystalline phases of He^3 and He^4) shows a thermodynamic behavior very similar to that of ordinary crystals. The calculated Debye temperatures are about 15–20% higher than those recently measured by Sample and Swenson. A possible cause for this discrepancy is indicated.

I. INTRODUCTION

CRYSTALS of the various isotopes of helium and molecular hydrogen cannot be treated by the "classical" theory of lattice dynamics.[1] This difficulty is due to the small mass of these substances and the weakness of the attractive part of their van der Waals interaction. Therefore, the quantum-mechanical zero-point energy in these crystals is comparable to their potential energy, and the root-mean-square (rms) deviation of a particle from its lattice site is not small compared to the nearest-neighbor distance. The problem is not simply that the anharmonic terms are large; it is that the harmonic approximation itself breaks down. This result has been demonstrated by de Wette and Nijboer,[2] who found that the traditional theory, when applied to crystalline helium, yields imaginary phonon frequencies at each point of the first Brillouin zone, so that the harmonic Hamiltonian is not Hermitian. Because of the failure of the traditional lattice-dynamics formulation for these solids owing to the relatively large zero-point motion, they have been called quantum crystals.[3]

In view of the existing experimental evidence regarding these crystals, the instability found from the classical theory may seem puzzling. After all, the crystals do exist and x-ray measurements[4] show that they have well-defined structures. In addition, the heat capacities have been extensively studied[5–7] and seem to be unusual only for bcc He^3 very near melting. Furthermore, sound velocity measurements[8,9] have yielded no surprises. It is true that these crystals have large compressibilities,[5,6,10] but the thermal expansion[11] seems quite normal, again except for bcc He^3 near melting. Thus the picture presented by the existing experimental results is that these crystals show no behavior quali-

* Based in part on work performed at the Argonne National Laboratory under the auspices of the U. S. Atomic Energy Commission. Also partially supported by the U. S. Air Force Office of Scientific Research under Grant Nos. AF-AFOSR 840-65 and AF-AFOSR 1257-67, and by the U. S. Atomic Energy Commission under contract No. AT(11-1) 1569.

[1] M. Born and K. Huang, *Dynamical Theory of Crystal Lattices* (Oxford University Press, London, 1956).

[2] F. W. de Wette and B. R. A. Nijboer, Phys. Letters **18**, 19 (1965).

[3] L. H. Nosanow, Phys. Rev. **146**, 120 (1966).

[4] A. F. Schuch, E. R. Grilly, and R. L. Mills, Phys. Rev. **110**, 775 (1958).

[5] E. C. Heltemes and C. A. Swenson, Phys. Rev. **128**, 1512 (1962).

[6] D. O. Edwards and R. C. Pandorf, Phys. Rev. **140**, A816 (1965).

[7] H. H. Sample and C. A. Swenson, Phys. Rev. (to be published).

[8] J. H. Vignos and H. A. Fairbank, in *Proceedings of the Eighth International Conference on Low-Temperature Physics, London, 1962*, edited by R. O. Davies (Butterworths Scientific Publications, Ltd., London, 1962); W. R. Abel, A. C. Anderson, and J. C. Wheatley, Phys. Rev. Letters **7**, 299 (1961).

[9] F. P. Lipschultz and D. M. Lee, Phys. Rev. Letters **14**, 1017 (1965).

[10] E. D. Adams, G. C. Straty, and E. L. Wall, Phys. Rev. Letters **15**, 549 (1965).

[11] J. F. Jarvis and H. Meyer, Bull. Am. Phys. Soc. **11**, 174 (1966).

tatively different from that of ordinary crystals which are adequately described by traditional lattice dynamics.

The theory which we present in this paper has as its objectives not only the calculation of various properties of these crystals from as fundamental a point of view as possible, but also the understanding of the basic physical reasons for their observed "mundane" behavior. A preliminary account of this work has already been published.[12] Our starting point is the Hartree approximation, in which the wave function of the crystal is written as a product of single-particle wave functions, each centered about a different lattice site. The virtue of the Hartree approximation is that it yields a self-consistent solution in which the particles are indeed localized, i.e., it is a convenient way to introduce the structure of the crystal into the calculation.

It is well known that the Hartree approximation does not treat the correlations in this system properly. In particular, we expect both short- and long-range correlations to be of importance in these crystals. The short-range effects are present because of the very strong short-range repulsion which exists between two atoms, whereas the long-range correlations are present because there must be collective motions (phonons) involving all of the particles.

We treat the phonons by means of the time-dependent Hartree approximation.[13] Here it is assumed that the system wave function in the presence of externally imposed disturbances may still be factorized for all times into a product of single-particle functions. With this assumption it is possible to calculate the response of the system to a weak space- and time-varying perturbation. In this way the phonon frequencies appear as poles of the response function in complete analogy with the way the collective excitations appear in the electron gas or in magnetic systems.[14]

We treat the short-range correlations by adopting the results of a variational calculation of the ground-state energy using cluster-expansion techniques.[3,15] This calculation assumes that the trial wave function is a product of single-particle functions times a product over all pairs of a two-particle function. The two-particle function is chosen to have a simple form which vanishes rapidly for small interparticle separations, thus avoiding the hard-core repulsion, and which contains a free parameter chosen so as to minimize the energy. It turns out that the single-particle function is the solution of the Hartree equation for a crystal but with the replacement of the true potential by an effective potential which no longer has a singular repulsion. Although this calculation yields ground-state energies which are about 10 cal/mole higher than experiment, it produces values for the pressure and compressibility which are accurate to about 10%.

In the present paper we synthesize the time-dependent Hartree and cluster-variational techniques to calculate the phonon frequencies of bcc He^3 and He^4. Our approach is simply to replace the potential in the time-dependent Hartree calculation by the effective potential deduced from the cluster-variational approach. A review of the necessary formal background and a derivation and discussion of our final formulas for the phonon frequencies are given in Sec. II. The results of the numerical evaluation of the frequencies are presented in Sec. III, in the form of dispersion curves, density of states, and low-temperature specific heat and mean square displacement. These results are assessed and discussed in Sec. IV, and in an Appendix we comment on the numerical procedures used in obtaining them.

II. FORMAL DEVELOPMENT

Reviewing the formal basis for our calculation of the phonon spectrum, we begin by summarizing the theory of Fredkin and Werthamer (FW) appropriate for a nonsingular interatomic potential. This theory regards the phonons as being among the set of normal modes of small-amplitude oscillation of the system about its equilibrium state. That is, the phonon frequency $\omega(\mathbf{k})$ is given by a pole of the response function of the system to an infinitesimal disturbance of wave number $\mathbf{k}$. The equilibrium state is approximated in an especially simple way, namely by the Hartree description, so that the time-dependent response about this equilibrium is just the familiar random-phase approximation (RPA). As is usual in the RPA, modes of different wave number do not interfere with each other, and hence the phonons are undamped to this approximation.

The Hartree representation for the equilibrium state (we specialize here to $T=0$) is a set of single-particle eigenfunctions $\varphi_\alpha(\mathbf{x})$ and eigenvalues Ω_α satisfying the self-consistent equation

$$\left[-(\hbar^2/2M)\nabla^2+\sum_{\tau\neq 0}\int d^3x'\ \varphi_0^2(\mathbf{x}')v(|\mathbf{x}-\mathbf{x}'+\boldsymbol{\tau}|)\right]\varphi_\alpha(\mathbf{x}) = \Omega_\alpha\varphi_\alpha(\mathbf{x}), \quad (1)$$

where $\boldsymbol{\tau}$ is a lattice vector, $\alpha=0$ is the lowest-energy state, and v is the interatomic potential taken to be of the Lennard-Jones type,

$$v(r)=4\epsilon[(\sigma/r)^{12}-(\sigma/r)^6]. \quad (2)$$

If we assume an infinitesimal disturbance which is applied with frequency ω and wave vector $\mathbf{k}$, and which couples to a one-particle observable $O(\mathbf{x})$, then FW

[12] L. H. Nosanow and N. R. Werthamer, Phys. Rev. Letters **15**, 618 (1965). We refer to this paper as NW.

[13] D. R. Fredkin and N. R. Werthamer, Phys. Rev. **138**, A1527 (1965). We refer to this paper as FW.

[14] See, e.g., R. H. Brout, *Phase Transitions* (W. A. Benjamin, Inc., New York, 1965).

[15] J. H. Hetherington, W. J. Mullin, and L. H. Nosanow, Phys. Rev. **154**, 175 (1967). We refer to this paper as HMN.

arrive at the formula for the response of O,

$$R(\mathbf{k},\omega)=\sum_{\alpha\alpha',\gamma\gamma'}\left[\int d^3x\ \varphi_\alpha(\mathbf{x})O(\mathbf{x})\varphi_{\alpha'}(\mathbf{x})\right]\times[\mathfrak{M}^{-1}(\mathbf{k},\omega)]_{\alpha\alpha',\gamma\gamma'}(\Omega_\gamma-\Omega_{\gamma'})(\delta_{\gamma',0}-\delta_{\gamma,0})\times\left[\int d^3x'\ \varphi_\gamma(\mathbf{x}')O(\mathbf{x}')\varphi_{\gamma'}(\mathbf{x}')\right], \quad (3)$$

with the matrix $\mathfrak{M}$ defined as

$$[\mathfrak{M}(\mathbf{k},\omega)]_{\alpha\alpha',\gamma\gamma'}\equiv\omega^2\delta_{\alpha,\gamma}\delta_{\alpha',\gamma'}-[\mathfrak{D}(\mathbf{k})]_{\alpha\alpha',\gamma\gamma'}, \quad (4)$$

$$[\mathfrak{D}(\mathbf{k})]_{\alpha\alpha',\gamma\gamma'}=(\Omega_\alpha-\Omega_{\alpha'})^2\delta_{\alpha,\gamma}\delta_{\alpha',\gamma'}-(\Omega_\alpha-\Omega_{\alpha'})\times(\delta_{\alpha,0}-\delta_{\alpha',0})N^{-1}\sum_\tau e^{-i\mathbf{k}\cdot\tau}\int d^3x d^3x'\ \varphi_\alpha(\mathbf{x})\varphi_\gamma(\mathbf{x}')\times v(|\mathbf{x}-\mathbf{x}'+\tau|)\varphi_{\alpha'}(\mathbf{x})\varphi_{\gamma'}(\mathbf{x}'). \quad (5)$$

Since we assume a Bravais lattice, N is the total number of particles in the system.

The poles of the response function, and hence the collective mode spectrum, are given by the zeros of $\mathfrak{M}(\mathbf{k},\omega)$. But since $\mathfrak{M}$ is a very large matrix, of dimensionality equal to the square of the number of eigenstates of the Hartree Eq. (1), it has an equally large number of zeros. The problem then arises as to which three (for given $\mathbf{k}$) are the phonon modes, a problem treated adequately by FW only for $\mathbf{k}=0$. The phonons are defined as those modes for which the response is nonvanishing when O is chosen to be an atomic displacement, $O(\mathbf{x})=\mathbf{x}$. The easiest way to proceed is to introduce the similarity transformation $\mathfrak{U}$ which diagonalizes $\mathfrak{D}$, so that

$$\sum_{\gamma\gamma'}[\mathfrak{D}(\mathbf{k})]_{\alpha\alpha',\gamma\gamma'}[\mathfrak{U}(\mathbf{k})]_{\gamma\gamma',\lambda}=\omega_\lambda^2(\mathbf{k})[\mathfrak{U}(\mathbf{k})]_{\alpha\alpha',\lambda}. \quad (6)$$

Then we can write

$$[\mathfrak{M}^{-1}(\mathbf{k},\omega)]_{\alpha\alpha',\gamma\gamma'}=\sum_\lambda[\omega^2-\omega_\lambda^2(\mathbf{k})]^{-1}\times[\mathfrak{U}(\mathbf{k})]_{\alpha\alpha',\lambda}[\mathfrak{U}^{-1}(\mathbf{k})]_{\lambda,\gamma\gamma'}. \quad (7)$$

Although we are unable to specify $\mathfrak{U}$ completely, we are at least able to exhibit three elements of the matrix

$$[\mathfrak{U}(\mathbf{k})]_{\alpha\alpha',\lambda}=(\Omega_\alpha-\Omega_{\alpha'})(\delta_{\alpha,0}-\delta_{\alpha',0})\times\int d^3x\ \varphi_\alpha(\mathbf{x})\mathbf{e}_{\mathbf{k}\lambda}\cdot\mathbf{x}\varphi_{\alpha'}(\mathbf{x}),$$

$$[\mathfrak{U}^{-1}(\mathbf{k})]_{\lambda,\alpha\alpha'}=\int d^3x\ \varphi_\alpha(\mathbf{x})\mathbf{e}_{\mathbf{k}\lambda}\cdot\mathbf{x}\varphi_{\alpha'}(\mathbf{x}), \quad (8)$$

$$\lambda=1,2,3,$$

with the $\mathbf{e}_{\mathbf{k}\lambda}$ being three orthonormal unit vectors which will turn out to be the phonon polarizations. Then using the dipole sum rules of FW, Eqs. (38) and (39), we find that Eq. (6) for $\lambda=1, 2, 3$ reduces to

$$\omega_\lambda^2(\mathbf{k})\mathbf{e}_{\mathbf{k}\lambda}=\frac{1}{MN}\sum_\tau(1-e^{-i\mathbf{k}\cdot\tau})\frac{\partial^2}{\partial\tau\partial\tau}\int d^3x d^3x'\ \varphi_0^2(\mathbf{x})\times\varphi_0^2(\mathbf{x}')v(|\mathbf{x}-\mathbf{x}'+\tau|)\cdot\mathbf{e}_{\mathbf{k}\lambda}. \quad (9)$$

Choosing the $\mathbf{e}_{\mathbf{k}\lambda}$ as eigenvectors of the tensor on the right-hand side in Eq. (9) is sufficient to guarantee that the $\mathfrak{U}$ elements exhibited in Eq. (8) indeed diagonalize $\mathfrak{M}$. Furthermore, noting Eq. (8), we find that the displacement-displacement response tensor given by Eq. (3) with $O(\mathbf{x})=\mathbf{x}$ can be re-expressed as

$$\mathbf{R}(\mathbf{k},\omega)=\sum_{\lambda,\lambda'=1}^{3}\mathbf{e}_{\mathbf{k}\lambda}\mathbf{e}_{\mathbf{k}\lambda'}\sum_{\alpha\alpha',\gamma\gamma'}[\mathfrak{U}^{-1}(\mathbf{k},\omega)]_{\lambda,\alpha\alpha'}\times[\mathfrak{M}^{-1}(\mathbf{k},\omega)]_{\alpha\alpha',\gamma\gamma'}[\mathfrak{U}(\mathbf{k},\omega)]_{\gamma\gamma',\lambda'}, \quad (10)$$

and so using Eq. (7),

$$\mathbf{R}(\mathbf{k},\omega)=\sum_{\lambda=1}^{3}\mathbf{e}_{\mathbf{k}\lambda}\mathbf{e}_{\mathbf{k}\lambda}[\omega^2-\omega_\lambda^2(\mathbf{k})]^{-1}. \quad (11)$$

Thus the three modes exhibited are the *only* ones which contribute to the displacement-displacement response, and thus are unambiguously identified as the one-phonon modes. Equation (9) is similar to the usual eigenvalue equation in the harmonic approximation but with the positions of the two interacting atoms averaged over their mean ground-state distribution. Equation (9) was the basis for the numerical work of Nosanow and Werthamer, but it was not recognized there or in FW to be the exact projection of Eq. (6) onto the one-phonon manifold.[16]

So far the discussion has been limited to nonsingular potentials, and hence cannot be applied directly to helium. To overcome this difficulty we look to the cluster-variational calculations[3,15] of the ground-state energy, where a trial ground-state wave function,

$$\Psi(\mathbf{x}_1,\cdots,\mathbf{x}_N)=\prod_i\varphi_0(\mathbf{x}_i-\mathbf{R}_i)\prod_{j<k}f(|\mathbf{x}_j-\mathbf{x}_k|), \quad (12)$$

was adopted, where $\mathbf{R}_i$ is the position of the ith lattice site. The correlation function f was chosen in a form to modify the hard-core region of the potential,

$$f(r)=\exp\{-K[(\sigma/r)^{12}-(\sigma/r)^6]\}, \quad (13)$$

and K was left free as a variational parameter. The expectation value of the Hamiltonian in this trial state was reduced to a manageable form by making a cluster expansion. With only two-body clusters retained,[3] the resulting trial ground-state energy was varied functionally with respect to φ_0, leading to an equation

[16] The development leading to the proofs of Eqs. (9) and (11) is due to Dr. N. S. Gillis, whom we thank for permission to quote these results.

generalizing Eq. (1) which was integrated numerically. The φ_0 so determined was well approximated by a Gaussian,

$$\varphi_0(\mathbf{x})\cong(A/\pi)^{3/4}\exp(-\tfrac{1}{2}Ax^2), \tag{14}$$

except for large x. Making use of result (14) in an alternative calculation,[15] we again adopted the wave function of Eq. (12), but φ_0 was restricted to a Gaussian in form with the parameter A left free. Then both two- and three-body clusters were retained and the parameters A and K were determined variationally. While the three-body cluster terms played a significant role in determining the minimum of the energy with respect to A, especially in the dependence on density, at the minimum the three-body clusters were approximately two orders of magnitude smaller than the two-body terms. Thus it is reasonable to conclude that the cluster expansion is converging rapidly for the choice of f given by Eq. (13).

The conclusions to be drawn from this work which are most relevant to the present calculations are that the single-particle ground-state wave function φ_0 is well approximated by a Gaussian, and that the predominant effect of the correlation function in determining φ_0 is to alter the interatomic potential appearing in Eq. (1) into an effective potential,

$$v\rightarrow W\equiv f^2[v-(\hbar^2/2M)\nabla^2\ln f]. \tag{15}$$

We have appealed to these results in justification of the heuristic modifications we have made in the phonon eigenvalue Eq. (9), namely the replacement of v by W together with the Gaussian approximation (14) for φ_0, where the parameters A and K are taken from the energy cluster-variational calculations.[15] Of course this procedure is rather arbitrary, because it implies the assumption that the short-range correlations, which cancel the effects of the hard core in v, are independent of the longer-range correlations which are involved in the phonon modes. This seems true for $k\sim0$, but our intuition might argue for a close interconnection between short-wavelength phonons and the correlated motions by which particles avoid strong hard-core interactions. Nevertheless, we feel that the procedure we have adopted is the simplest one which removes spurious hard-core effects in a reasonable manner.

With these modifications—the use of the effective potential (15) and the Gaussian single-particle wave function approximation (14)—the integrations in Eq. (9) can be reduced to a one-dimensional form, so that

$$\omega_\lambda^2(\mathbf{k})\mathbf{e}_{\mathbf{k}\lambda}=\frac{1}{MN}\sum_{\boldsymbol{\tau}}(1-\cos\mathbf{k}\cdot\boldsymbol{\tau})\frac{\partial^2}{\partial\boldsymbol{\tau}\partial\boldsymbol{\tau}}\left\{\left(\frac{A}{2\pi}\right)^{1/2}\frac{1}{\tau}\int_0^\infty dr\, rW(r)[\exp(-\tfrac{1}{2}A(r-\tau)^2)-\exp(-\tfrac{1}{2}A(r+\tau)^2)]\right\}\cdot\mathbf{e}_{\mathbf{k}\lambda}. \tag{16}$$

Equation (16) is the final expression which has been programmed for numerical evaluation.

Since it is to be expected that these crystals can, at sufficiently low temperatures, be described in terms of noninteracting elementary excitations, it should be a good approximation to calculate the specific heat per particle using the elementary formula

$$C_V=\frac{k_B}{N}\sum_{\mathbf{k},\lambda}\frac{[\hbar\omega_\lambda(\mathbf{k})/k_BT]^2\exp[-\hbar\omega_\lambda(\mathbf{k})/k_BT]}{\{1-\exp[-\hbar\omega_\lambda(\mathbf{k})/k_BT]\}^2}, \tag{17}$$

with the frequencies computed from Eq. (16). Unfortunately, this formula does not follow in any direct way from the RPA, since the phonon spectrum in the RPA only enters into the response function and not into the equilibrium properties. The free energy can be expressed formally in terms of the displacement-displacement response as in Eq. (53) of FW, but this involves a mass integration at fixed density. This formulation fails for bcc helium, because for large masses the frequencies become imaginary.[2] At temperatures for which the elementary excitations begin to interact, there is a correction to Eq. (17) due to the temperature dependence of the phonon frequencies. However, it is to be expected[17] that this correction will be smaller by a factor of the order of $(T/\Theta_D)^4$, and will be negligible for crystalline helium which melts at $T/\Theta_D\sim0.1$.

III. PRESENTATION OF RESULTS: He^3

A. Phonon Frequencies

The squares of the phonon frequencies $\omega_\lambda(\mathbf{k})$ are the roots of the secular equation of Eq. (16), namely

$$\det\left|\omega_\lambda^2(\mathbf{k})\delta_{\xi,\xi'}-\frac{1}{MN}\sum_{\boldsymbol{\tau}}(1-\cos\mathbf{k}\cdot\boldsymbol{\tau})\times\frac{\partial^2}{\partial\tau_\xi\partial\tau_{\xi'}}g(|\boldsymbol{\tau}|)\right|=0, \tag{18}$$

where ξ and ξ' stand for x, y, and z, and

$$g(|\boldsymbol{\tau}|)=\left(\frac{A}{2\pi}\right)^{1/2}\frac{1}{\tau}\int_0^\infty dr\, rW(r)\{\exp[-\tfrac{1}{2}A(r-\tau)^2]-\exp[-\tfrac{1}{2}A(r+\tau)^2]\}. \tag{19}$$

Equation (18) has initially been solved for a coarse mesh of 5525 different $\mathbf{k}$ vectors distributed uniformly over the irreducible part (1/48) of the Brillouin zone (BZ) of the bcc lattice. This has been done for the four densities of bcc He^3 (corresponding to the molar volumes $V_m=19.0$, 20.7, 22.5, and 24.5 cm^3) for which the Gaussian single-particle wave function φ_0 has been determined by Hetherington, Mullin, and Nosanow (HMN).[15]

[17] J. I. Kaplan, Phys. Letters **17**, 227 (1965).

Various results that are immediately obtained from these calculations are presented in Figs. 1 through 9. In Figs. 1, 2, and 3 we have plotted the dispersion curves $\omega_\lambda(\mathbf{k})$ along the [ζ00], [ζζ0], and [ζζζ] directions and their connections along the zone boundary, for the highest density considered ($V_m = 19.0$ cm^3). In Figs 4, 5, and 6 we give the same curves for the lowest density ($V_m = 24.5$ cm^3). Note that these dispersion curves have the familiar shape that is characteristic for monatomic bcc lattices.

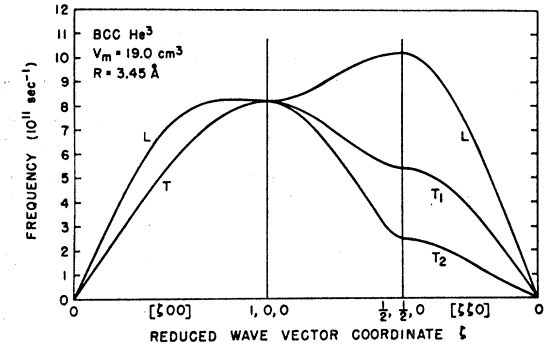

FIG. 1. Phonon dispersion curves for bcc He³ at molar volume of 19.0 cm³, along the directions [ζ00], [ζζ0], and the connecting line on the zone surface. (L and T refer to the longitudinal and transverse branches, respectively.)

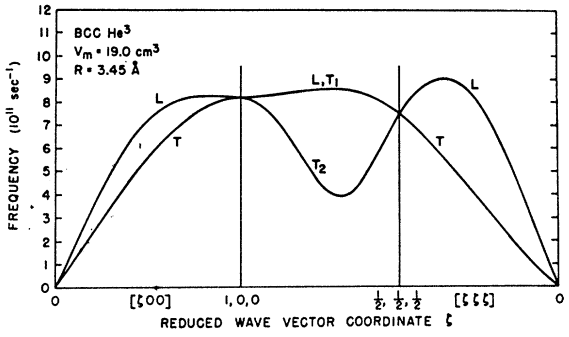

FIG. 2. Phonon dispersion curves for bcc He³ at molar volume of 19.0 cm³, along the directions [ζ00], [ζζζ], and the connecting line on the zone surface.

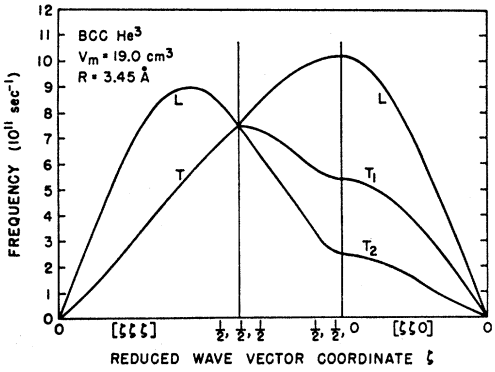

FIG. 3. Phonon dispersion curves for bcc He³ at molar volume of 19.0 cm³, along the directions [ζζζ], [ζζ0], and the connecting line on the zone surface.

In Figs. 7 and 8 we present the longitudinal and transverse sound velocities in the various symmetry directions as functions of the molar volume (solid lines).

For comparison the earlier results of Nosanow and Werthamer[12] are shown (dashed lines), which were based on a less accurate Gaussian φ_0. In Fig. 7 the experimental results[8] have also been indicated. These Figs. 7 and 8 have been taken directly from HMN, on whose results for φ_0 our calculations have been based.

Finally, in Figs. 9 and 10 we have plotted the histograms of the density of states for the highest and lowest densities. Like the dispersion curves, these histograms

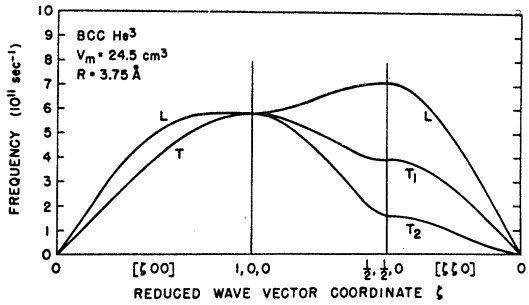

FIG. 4. Phonon dispersion curves for bcc He³ at molar volume of 24.5 cm³, along the directions [ζ00], [ζζ0], and the connecting line on the zone surface.

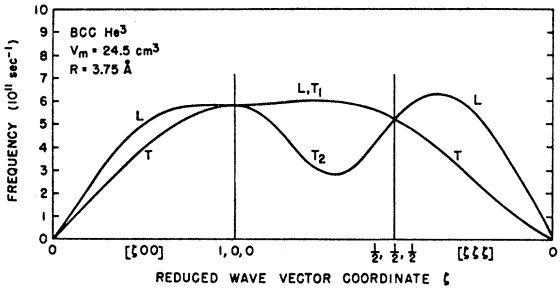

FIG. 5. Phonon dispersion curves for bcc He³ at molar volume of 24.5 cm³, along the directions [ζ00], [ζζζ], and the connecting line on the zone surface.

have a shape that is characteristic for a monatomic bcc lattice. The resolution in these histograms is rather limited, because in obtaining them, we have only used the frequencies calculated for the coarse $\mathbf{k}$ mesh (see below), and we have not made use of knowledge about the location of critical points.

Experimental data in regard to the phonon spectrum are very limited; no inelastic neutron scattering experiments have been carried out on helium, and sound-velocity measurements only exist for unoriented crystals.

B. Thermodynamic Quantities

The thermodynamic quantities that are of most interest to calculate, once the phonon frequencies are

known, are the specific heat at constant volume, and the mean square displacement of the particles, which figures directly into the Debye-Waller factor. It gives the most direct measure of the large zero-point vibrations which exist in solid helium.

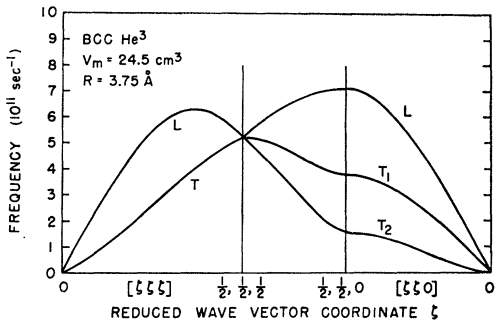

FIG. 6. Phonon dispersion curves for bcc He^3 at molar volume of 24.5 cm^3, along the directions $[\zeta\zeta\zeta]$, $[\zeta\zeta 0]$, and the connecting line on the zone surface.

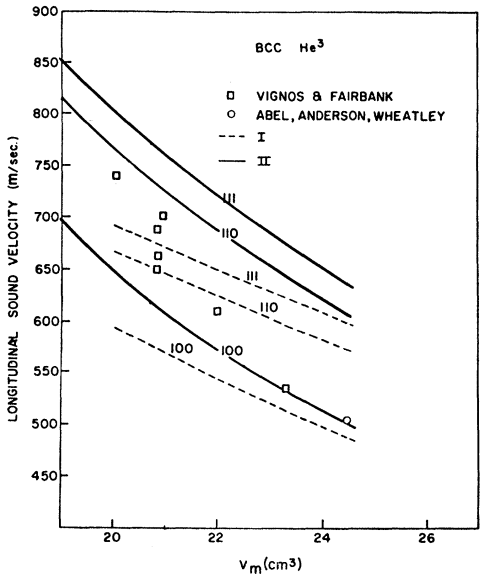

FIG. 7. Longitudinal sound velocities in symmetry directions as a function of molar volume. Solid curves are the present results; dashed curves are the previous results of Nosanow and Werthamer (Ref. 12) using less accurate variational parameters in the Gaussian single-particle wave functions. Measurements of Vignos and Fairbank, and of Abel, Anderson, and Wheatley, on unoriented crystals are indicated.

The mean square displacement, which we discuss first, is given by the expression[18]

$$\langle u^2\rangle=\frac{\hbar}{2NM}\sum_{\mathbf{k},\lambda}\frac{\coth[\hbar\omega_\lambda(\mathbf{k})/2k_BT]}{\omega_\lambda(\mathbf{k})}, \qquad (20)$$

and is closely related to the Debye-Waller factor for scat-

[18] See, e.g., A. A. Maradudin, E. W. Montroll, and G. M. Weiss, *Theory of Lattice Dynamics in the Harmonic Approximation* (Academic Press Inc., New York, 1963), Chap. VII.

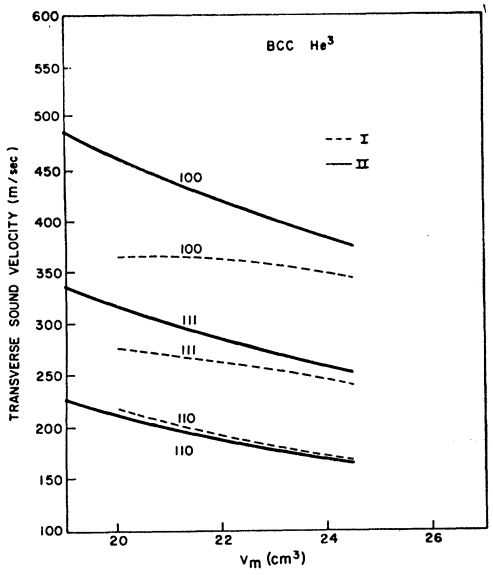

FIG. 8. Transverse sound velocities in symmetry directions as a function of molar volume. Solid curves are the present results; dashed curves are the previous results of Nosanow and Werthamer (Ref. 12) using less accurate variational parameters in the Gaussian single-particle wave functions.

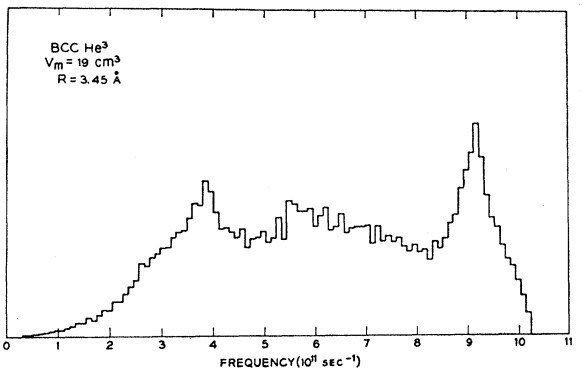

FIG. 9. Histogram of the phonon density of states of bcc He^3 at molar volume of 19.0 cm^3.

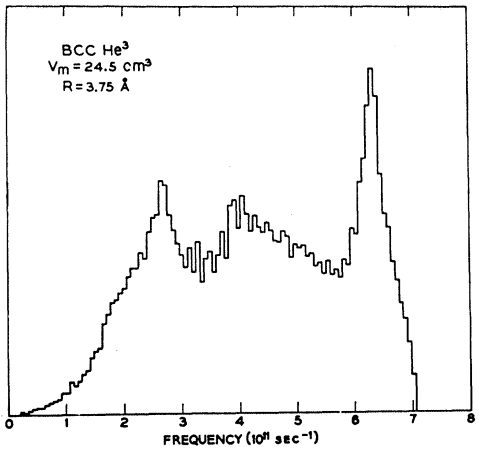

FIG. 10. Histogram of the phonon density of states of bcc He^3 at molar volume of 24.5 cm^3.

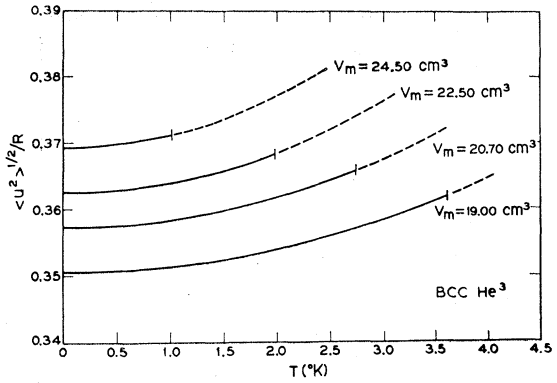

FIG. 11. rms atomic displacements in bcc He^3 normalized to the nearest-neighbor distance, as a function of temperature at four different molar volumes.

tering with momentum transfer $\mathbf{K}$, viz., $\exp[-2W(\mathbf{K})]$. For cubic crystals W has the simple form

$$W(\mathbf{k})=\frac{2\pi^2K^2}{3}\langle u^2\rangle. \tag{21}$$

In Fig. 11 we have plotted the quantity $\langle u^2\rangle^{1/2}/R$, i.e., the rms displacement divided by the nearest-neighbor distance, as a function of temperature. The melting temperature in each case has been indicated by a vertical bar.

The large values of $\langle u^2\rangle^{1/2}/R$ at absolute zero give a quantitative confirmation of the long-known fact that the zero-point amplitudes in solid helium, especially at large molar volumes (lowest pressures), are very large. We further note that the mean-square displacement increases by only a small fraction of its zero-point value before melting takes place, as is especially evident for $V_m=24.5$ cm³. This illustrates the point, made long ago by London,[19] that melting of solid helium at low pressures is predominantly a mechanical effect. This is also immediately evident from the fact that the thermal energy at melting is only a small fraction of the zero-point energy at these low pressures and temperatures.

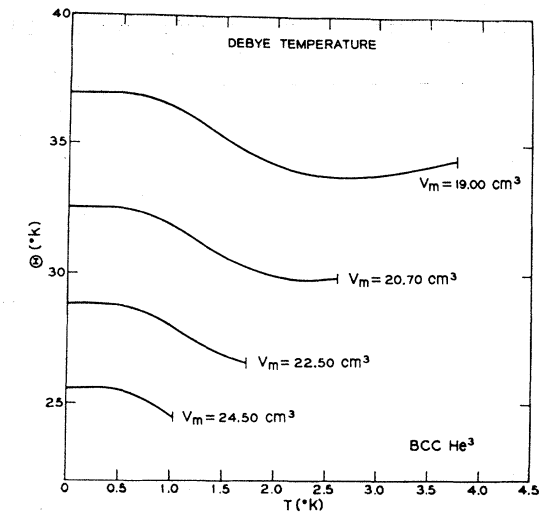

FIG. 12. The Debye temperature of bcc He^3 as a function of temperature, at four different molar volumes.

We also present the results obtained for the specific heat C_V. The numerical procedures used to obtain these results are discussed in the Appendix. In Fig. 12 we have expressed the specific-heat results in terms of the temperature-dependent Debye temperature $\Theta(T)$ for the four molar volumes considered. The limiting values $\Theta_0=\Theta(0)$ are given in Table I.

In Fig. 13 we present $\Theta(T)$ curves (solid lines) for the same molar volumes for which specific-heat measurements have recently been carried out by Sample and Swenson[7] (indicated by the dashed lines). Our results were obtained by interpolation from the data presented in Fig. 12.

The main difference between the experimental and the theoretical curves is that the latter give larger Debye temperatures (i.e., smaller specific heats) and are much less temperature-dependent.

The experimental curves for $\Theta(T)$ exhibit a sharp drop at low temperatures and a somewhat less sharp decline at high temperatures. Both features are manifestations of anomalous contributions to the specific heat in these temperature ranges, the origins of which are still unknown, although it has been suggested that the high-temperature anomaly is caused by creation of lattice imperfections.[20,21] In order to avoid the low-temperature anomaly, Sample and Swenson have chosen to identify the maxima in the experimental $\Theta(T)$ curves as representing the zero temperature Θ_0's of the true lattice specific heat. If this is a correct procedure, then there exists an important discrepancy (of order 15–20%) between theoretical and experimental Debye temperatures Θ_0 which we are unable to explain. Other quantities calculated with this theory, such as ground-state energy and compressibility, are typically accurate to about 10%. However, the possibility cannot be excluded that at the maxima of the experimental $\Theta(T)$ curves the low-temperature as well as the high-temperature anomalous contributions to the specific heat are both present to some extent. In that case the

TABLE I.

Molar volume in cm³	Nearest-neighbor distance in Å	Θ_0 in °K
19.0	3.45	36.92
20.7	3.55	32.54
22.5	3.65	28.84
24.5	3.75	25.61

[19] F. London, *Superfluids* (Dover Publications, Inc., New York, 1950), Vol. II.
[20] D. O. Edwards, A. S. McWilliams, and J. G. Daunt, Phys. Letters **1**, 218 (1962).
[21] F. W. de Wette, Phys. Rev. **129**, 1160 (1963).

true lattice Θ_0 would be larger than that derived by the procedure of Sample and Swenson, and part of the discrepancy would be removed. It should also be noted that the theoretical Θ_0 values quoted here differ by about 10% from those obtained earlier by HMN, although the sound velocities are virtually identical. We attribute this to use by HMN, and also by NW, of a simple Houston's interpolation method for approximating an angular average over $\mathbf{k}$ space from values computed along just three symmetry directions.

Finally, in Fig. 14 we have plotted the reduced Θ-T relationship [i. e., $\Theta(T)/\Theta_0$ versus T/Θ_0] for the lattice specific heat of bcc He^3. It turns out that for all densities considered, these reduced Θ-T relationships follow one universal curve with an accuracy of about $\frac{1}{10}$%. This important result is yet another manifestation of the completely classical behavior of the lattice specific heat of solid He^3. In addition, the existence of this universal Θ-T relationship enables one to subtract from the measured specific heat what we believe to be a reasonable estimate of the lattice contribution, so that the part of the high-temperature specific heat of bcc He^3 which is anomalous can be more accurately determined. We intend to carry out this reduction of the experimental data in a future article.

IV. PRESENTATION OF RESULTS: He^4

The calculations on He^3 described in the previous section have also been carried out for bcc He^4 at the density of $V_m=21.0$ cm^3. However, we find that the results are all so close (within 1%) to those for He^3 at $V_m=24.5$ cm^3 that we do not show any of these separately here.

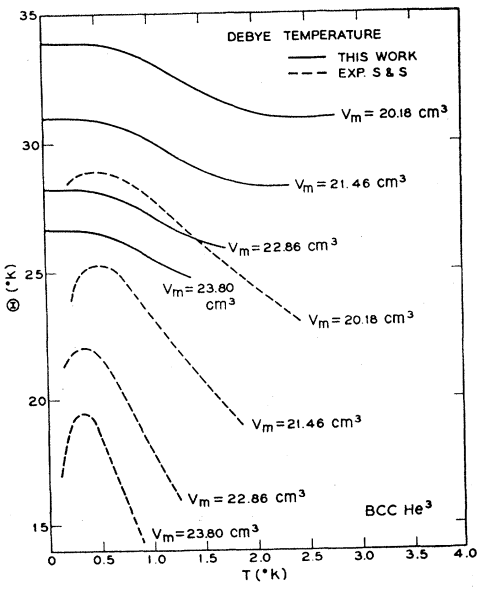

FIG. 13. Debye temperature of bcc He^3 (solid curves) as a function of temperature, interpolated from the results of Fig. 12 to the molar volumes appropriate to the data of Sample and Swenson (Ref. 7) (dashed curves).

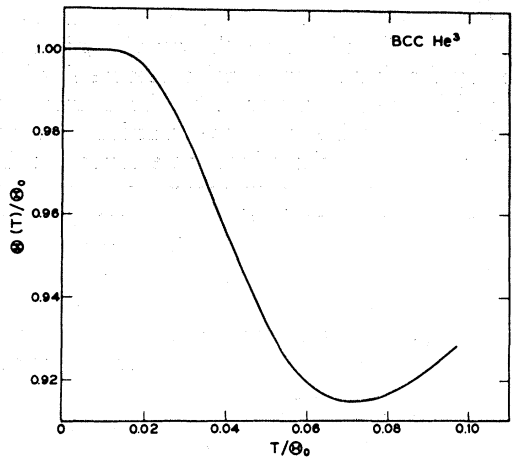

FIG. 14. A reduced plot of the Debye temperature of bcc He^3 as a function of temperature. All four molar volumes coincide to within the width of the line drawn.

V. DISCUSSION

If a comparison is made between the dispersion curves and density-of-states histograms for ordinary bcc crystals[22] and those which we have calculated for bcc He^3, it is immediately apparent that there are no qualitative differences. Thus our calculations agree with experiment in the sense that they yield an entirely conventional excitation spectrum. The mathematical reason for this result is that Eq. (9) is just the traditional eigenvalue equation for the phonon spectrum, but with the usual factor $v(\tau)$ replaced by the factor

$$\int d^3x d^3x' \; \varphi_0^2(\mathbf{x})\varphi_0^2(\mathbf{x}')v(|\mathbf{x}-\mathbf{x}'+\boldsymbol{\tau}|)$$

in our expression. One may look upon this change as replacing the force constants of the harmonic approximation by a new set of force constants which allow for the large zero-point motion of the individual atoms. It is just this zero-point motion which expands the crystal to its observed density. The two expressions become equal in the limit that the particles are fixed to their equilibrium positions.

One might have anticipated that the only change in the equation for the frequencies would be the alteration of the force constants. After all, excitations whose wavelengths are long compared to the nearest-neighbor distance should hardly be affected by the zero-point motion of the helium atoms whose amplitude is comparable to the nearest-neighbor distance. Furthermore, many of the features of the excitation spectrum are determined primarily by geometric considerations.

[22] See, e.g., *Lattice Dynamics*, edited by R. F. Wallis (Pergamon Press, Oxford, England, 1965).

The importance of including the effective interaction $W(r)$ in Eq. (16) and of using the wave functions determined by the cluster-variational procedure should also be noted. If we had merely used the Lennard-Jones potential and the Hartree wave functions, we would have found frequencies which were much too high. This is because the uncompensated hard cores would keep the particles too localized, so that the kinetic energy would be too large, and the crystal would be much too stiff. In contrast, the cluster-variational calculations[15] have produced compressibilities which agree with experiment to within approximately 10%, so that it is reasonable to assume that our phonon frequencies should be at least as accurate.

We should also like to point out that the phonon eigenvalue Eq. (9) based on the RPA resembles a formula recently obtained by Koehler[23] from a strict variational technique. In that work, the trial ground state of the system is selected to be a correlated Gaussian,

$$\Psi(\mathbf{x}_1,\cdots,\mathbf{x}_N) \propto \exp[-\tfrac{1}{2}\sum_{i,j}(\mathbf{x}_i-\mathbf{R}_i)\cdot\mathbf{G}_{ij}\cdot(\mathbf{x}_j-\mathbf{R}_j)], \quad (22)$$

which is also the exact ground state of some harmonic Hamiltonian whose dynamical matrix is related to $\mathbf{G}$. Varying the energy of this state with respect to all independent elements of $\mathbf{G}$ leads to a determination of the optimum such dynamical matrix, whose eigenvalue equation is

$$\omega_\lambda^2(\mathbf{k})\mathbf{e}_{\mathbf{k}\lambda}=\frac{1}{MN}\sum_{\tau}[1-(\exp-i\mathbf{k}\cdot\boldsymbol{\tau})] \times\frac{\partial^2}{\partial\boldsymbol{\tau}\partial\boldsymbol{\tau}}\langle v(|\mathbf{x}-\mathbf{x}'+\boldsymbol{\tau}|)\rangle\cdot\mathbf{e}_{\mathbf{k}\lambda}. \quad (23)$$

The difference from Eq. (9) is that here the expectation value is taken with respect to the *harmonic phonon* ground state, so that the phonon frequencies are determined self-consistently. Equation (23) is also quoted by Ranninger[24] as having been obtained by Choquard[25] using a perturbation expansion–resummation method. The physical difference between this formula and Eq. (9) is that the latter takes account of the mean probability distribution of the interacting particles due to the *single-particle* aspects of their motion, while the former attributes the probability distribution to the *collective* aspects of the motion. At the present time, it is not clear whether Eq. (9), Eq. (23), or some synthesis of the two is the most accurate description of the phonon frequencies.

[23] T. R. Koehler, Phys. Rev. Letters **17**, 89 (1966).
[24] J. Ranninger, Phys. Rev. **140**, A2031 (1965).
[25] P. Choquard, *Selected Topics in Lattice Dynamics* (W. A. Benjamin, Inc., New York, to be published).

ACKNOWLEDGMENTS

It is a pleasure to acknowledge helpful discussions with Dr. N. S. Gillis and to recognize his contributions to the derivation of Eqs. (9) and (11). We have benefited from conversations with Dr. T. R. Koehler and with Professor C. A. Swenson, and want to thank them for communicating their results in advance of publication. We would also like to thank Paul Steinback for programming assistance and the Numerical Analysis Center of the University of Minnesota, the Applied Mathematics Division of the Argonne National Laboratory, and the Computation Center of the University of Texas for their cooperation. One of the authors (F. W. de W.) wishes to thank the Graduate School of the University of Texas for a grant which made it possible for him to complete this research.

APPENDIX: NUMERICAL PROCEDURE FOR CALCULATING SPECIFIC HEATS

In principle the specific heat $C_V(T)$ is obtained by carrying out the $\mathbf{k}$ summation in Eq. (17) over the $\mathbf{k}$ mesh for which the phonon frequencies $\omega_\lambda(\mathbf{k})$ have been evaluated. However, for crystals at very low temperatures one encounters a particular difficulty, caused by the discreteness of the $\mathbf{k}$ mesh. Since the mesh is finite, there exists a smallest frequency, $\omega_{\min}$ in the calculated spectrum. For temperatures smaller than $\hbar\omega_{\min}/k_B$, the specific heat as calculated with (17), becomes anomalously small as a result of the exponential in the numerator. In order to obtain the C_V at the lowest temperature of interest (which happen to lie well below $\hbar\omega_{\min}/k_B$), a special procedure has to be followed.

It turns out that the original coarse $\mathbf{k}$ mesh of 5525 points in the irreducible part of the BZ is quite insufficient for the calculation of C_V at the temperatures of interest. In order to remedy this, however, it is not necessary to refine the $\mathbf{k}$ mesh throughout the entire zone. It sufficies to increase the mesh density towards the center of the BZ, since at lower temperatures the inner parts of the zone give the main contribution to C_V. Accordingly we have used three different $\mathbf{k}$ meshes, each containing 5525 points: a coarse mesh covering the entire zone, an intermediate mesh covering the inner 1/27 of the zone (linear dimensions $\frac{1}{3}$ of the coarse mesh), and a fine mesh covering the inner 1/729 of the zone (linear dimensions $\frac{1}{9}$ of the coarse mesh). Even these three meshes are insufficient to give accurate values for the specific heat of helium for temperatures below about 0.5°K. A further refinement of the $\mathbf{k}$ mesh, however, is unnecessary because the difficulties now occur in the linear dispersion region where the Debye approximation is strictly valid. With this in mind we have devised the following numerical procedure.

The quantity C_V that we wish to evaluate may be

expressed in the following form

$$S(T^*)=\frac{1}{N}\sum_{\mathbf{k},\lambda} f\left(\frac{\Omega_\lambda(\mathbf{k})}{T^*}\right) \tag{A1}$$

[cf. Eq. (17)]. Here T^* is a dimensionless temperature, $\Omega_\lambda(\mathbf{k})$ a dimensionless frequency, and

$$f(x)\equiv\frac{x^2e^{-x}}{(1-e^{-x})^2}. \tag{A2}$$

Our first step is to select three constant-Ω surfaces in the BZ, defined by $\Omega_\lambda(\mathbf{k})=\Omega^0$ ($\lambda=1,2,3$), where Ω^0 is a fixed frequency lying in the linear dispersion region in all directions.[26] We can now divide the $\mathbf{k}$ summation in (A1) into two parts, one over the $\mathbf{k}$ values for which $\Omega_\lambda(\mathbf{k})\leq\Omega^0$, and the other for $\mathbf{k}$ values for which $\Omega_\lambda(\mathbf{k})>\Omega^0$. We thus have

$$\begin{aligned}S(T^*)=&\frac{1}{N}\sum_\lambda\sum_{\mathbf{k},[\Omega_\lambda(\mathbf{k})\leq\Omega^0]} f\left(\frac{\Omega_\lambda(\mathbf{k})}{T^*}\right)\\&+\frac{1}{N}\sum_\lambda\sum_{[\mathbf{k},\Omega_\lambda(\mathbf{k})>\Omega^0]} f\left(\frac{\Omega_\lambda(\mathbf{k})}{T^*}\right)\\\equiv&S_1(T^*)+S_2(T^*).\end{aligned} \tag{A3}$$

At this point we recall that, theoretically, the $\mathbf{k}$ summations in (A1) and (A3) have to be carried out over the full $\mathbf{k}$ mesh, containing as many points as there are unit cells in the crystal ($\approx10^{23}$). In the numerical evaluation of S_2 the $\mathbf{k}$ summations are straightforwardly carried out over the sampling meshes described above, i.e., the outer mesh, the intermediate mesh, and the part of the fine mesh lying outside the constant-Ω surfaces. Of course, the contributions of these meshes have to be weighted properly, but this poses no special problems.

The $\mathbf{k}$ summations in S_1 (one for each λ), which are still to be taken over the full $\mathbf{k}$ mesh, may be replaced by $\mathbf{k}$ integrations over those parts of $\mathbf{k}$ space enclosed, respectively, by the three constant-energy surfaces. Using the identity $\sum_\mathbf{k}\to V\int d^3k$ we have

$$\begin{aligned}S_1(T^*)=&\frac{V}{N}\sum_\lambda\int_{[\Omega_\lambda(\mathbf{k})\leq\Omega^0]} d^3k\, f\left(\frac{\Omega_\lambda(\mathbf{k})}{T^*}\right)\\=&\frac{V}{N}\sum_\lambda\int\int\sin\theta d\theta d\varphi\int_0^{k_\lambda^0(\theta,\varphi)} dk\\&\times k^2 f\left(\frac{\Omega_\lambda(\mathbf{k})}{T^*}\right),\end{aligned} \tag{A4}$$

where k, θ, and φ are the polar coordinates of $\mathbf{k}$, and where $k_\lambda^0(\theta,\varphi)$ is determined by the relation

$$\Omega_\lambda[k_\lambda^0(\theta,\varphi)]=\Omega^0. \tag{A5}$$

However, in the linear dispersion region we have

$$\Omega_\lambda(\mathbf{k})=kS_\lambda(\theta,\varphi), \tag{A6}$$

$S_\lambda(\theta,\varphi)$ being the sound velocity of the polarization branch λ in the direction (θ,φ). Changing the integration variable from k to $x=\Omega_\lambda(\mathbf{k})/T^*$ we obtain

$$\begin{aligned}S_1=&\frac{V}{N}\sum_\lambda\int\int\sin\theta d\theta d\varphi\\&\times\left(\frac{T^*}{S_\lambda(\theta,\varphi)}\right)^3\int_0^{\Omega^0/T^*} dx\,x^2f(x).\end{aligned} \tag{A7}$$

Since, according to (A5) and (A6), $k_\lambda^0(\theta,\varphi)S_\lambda(\theta,\varphi)=\Omega^0$, (A7) may be written as

$$\begin{aligned}S_1=&\frac{V}{N}\sum_\lambda\int\int\sin\theta d\theta d\varphi\,[k_\lambda^0(\theta,\varphi)]^3\\&\times\left(\frac{T^*}{\Omega^0}\right)^3\int_0^{\Omega^0/T^*} dx\,x^2f(x).\end{aligned} \tag{A8}$$

The two integrals are independent of one another. Substituting the expression (A2) for $f(x)$ we note that the second integral,

$$J\left(\frac{T^*}{\Omega^0}\right)\equiv3\left(\frac{T^*}{\Omega^0}\right)^3\int_0^{\Omega^0/T^*}\frac{x^4e^{-x}}{(1-e^{-x})^2}dx, \tag{A9}$$

is closely related to one of the Debye functions.[27,28] Furthermore, it is easy to show that

$$V_\lambda\equiv\frac{1}{3}\int\int\sin\theta d\theta d\varphi\,[k_\lambda^0(\theta,\varphi)]^3 \tag{A10}$$

is the volume in $\mathbf{k}$ space enclosed by the constant-energy surface $\Omega_\lambda(\mathbf{k})=\Omega^0$. We thus arrive at the very simple expression for S_1:

$$S_1(T^*)=\frac{V}{N}J\left(\frac{T^*}{\Omega^0}\right)\sum_\lambda V_\lambda. \tag{A11}$$

If we had chosen a different constant-energy surface for each of the three polarization branches, we would have obtained the expression

$$S_1(T^*)=\frac{V}{N}\sum_\lambda J\left(\frac{T^*}{\Omega_\lambda{}^0}\right)V_\lambda. \tag{A12}$$

[26] Ω^0 may be chosen differently for different λ. However, for simplicity of the presentation we have chosen one single Ω^0 here.

[27] See, e.g., *Handbook of Mathematical Functions*, edited by M. Abramowitz, and I. A. Stegun (U. S. Department of Commerce, National Bureau of Standards, Washington, D. C., 1965), Appl. Math. Ser. 55.

[28] H. C. Thacher, Jr., J. Chem. Phys. **32**, 638 (1960).

It is evident that the evaluation of S_1 in either of these expressions has become exceedingly simple. In the form (A11) one has to evaluate only one single integral for each temperature T^*, while the form (A12) contains only three integrals. The volumes V_λ are easily obtained by adding up the elementary volumes associated with those $\mathbf{k}$ points of the fine mesh, which are omitted in the evaluation of S_2.

We conclude the Appendix by quoting two rational approximations for the integral $J(1/x)$ (A9). From Thacher's work[28] we derive that for the range $0 \leq x < 10$, $J(1/x)$ is very accurately approximated by the expression

$$\frac{3xe^{-x}}{e^{-x}-1}+4\left\{\frac{3953.632-800.6087x+85.07724x^2-4.43582x^3+0.0946173x^4}{3953.632+682.0012x+143.1553x^2+15.12149x^3+x^4}\right\}, \tag{A13}$$

in which the absolute error is smaller than 2.1×10^{-6}. For $x \geq 10$ we have used the expression

$$\frac{3xe^{-x}}{e^{-x}-1}+\frac{12}{x^3}\left[\frac{\pi^4}{15}-e^{-x}\{6+6x+3x^2+x^3\}\right], \tag{A14}$$

in which the fractional error is not larger than 5×10^{-6}. Expression (A14) has been obtained from a series expansion of the appropriate Debye function.[27]

PHYSICAL REVIEW VOLUME 162, NUMBER 3 15 OCTOBER 1967

Polariton Spectrum of α-Quartz

J. F. SCOTT, L. E. CHEESMAN, AND S. P. S. PORTO
Bell Telephone Laboratories, Murray Hill, New Jersey
(Received 11 May 1967)

Mixed electromagnetic-mechanical excitations known as "polaritons" are observed in Raman forward-scattering experiments on α-quartz using an argon laser. Dispersion relations of the polariton frequencies are extended from the case of simple diatomic lattices to a more complex system, namely, α-quartz, which has nine atoms per unit cell. The dependence of frequency upon scattering angle observed for these mixed excitations in quartz is shown to be in very good agreement with that predicted. Polaritons associated with the transverse phonons at 1072, 797, and 450 cm^{-1} in α-quartz are discussed in the present work. The polariton associated with the 1072-cm^{-1} phonon mode is observed to range in frequency from 1072 to 822 cm^{-1}; the polariton associated with the 797-cm^{-1} phonon mode is observed at frequencies from 797 to 700 cm^{-1}; and that associated with the 450-cm^{-1} phonon mode is observed from 450 to 407 cm^{-1}.

INTRODUCTION

In the study of the optical properties of solids much interest is currently focused on the nature of interactions between optical phonons and other crystalline excitations. Among these are interactions between phonons and plasmons, phonons and cyclotron resonance excitations, and phonons and photons. Until now the study of these interactions has been almost entirely restricted to simple crystals possessing diatomic lattice structure and a single phonon mode.[1] In the present work we consider phonon-photon coupling in α-quartz, which has nine atoms per unit cell and eight TO phonons of species E which can couple with photons travelling through the crystal.

Transverse optical phonons in polar crystals interact strongly with electromagnetic waves when their energies and momentum vectors are nearly equal. The resulting mixed excitations, called "polaritons" by Hopfield,[2] were first observed in Raman experiments on cubic GaP by Henry and Hopfield[3] and on hexagonal ZnO by Tell *et al.*,[4] who made use of the uniaxial properties of the latter crystal to produce large shifts in the frequency of the excitation. A general theoretical discussion of polaritons has been given recently by Hopfield.[5]

While both GaP and ZnO have diatomic lattice structure with only one TO branch, the polariton effect is also expected in more complicated crystals. In the

[1] An exception is Barker's work on phonon-plasmon effects in $SrTiO_3$. A. S. Barker, Jr., in *Proceedings of the Internal Colloquium on Optical Properties and Electronic Structure of Metals and Alloys, Paris, 1965* (North-Holland Publishing Company, Amsterdam, 1966).

[2] J. J. Hopfield, Phys. Rev. **112**, 1555 (1958).

[3] C. H. Henry and J. J. Hopfield, Phys. Rev. Letters **15**, 964 (1965).

[4] S. P. S. Porto, B. Tell, and T. C. Damen, Phys. Rev. Letters **16**, 450 (1966).

[5] J. J. Hopfield, in Kyoto Semiconductor Conference, Kyoto, Japan, 1966 (unpublished).